LIGHT-WEIGHT HYDRIDE DEVELOPMENT

K. J. Gross, G. J. Thomas, E. Majzoub and G. Sandrock
Sandia National Laboratories
Livermore, CA 94550

Abstract

The discovery that hydrogen can be reversibly absorbed and desorbed from complex hydrides (the alanates) by the addition of catalysts has created an entirely new prospect for lightweight hydrogen storage. These materials offer the possibility to achieve our program goal, which is to develop lightweight materials for onboard hydrogen storage in PEM fuel cell vehicles. Previous work concentrated on identifying both the positive and negative aspects of using catalyzed alanates as a practical means of storing hydrogen. We began by investigating the hydrogen storage properties of $NaAlH_4$ mechanically doped with 2 mol% each of the liquid alkoxides $Ti(OBu^n)_4$ + $Zr(OPr)_4$ catalysts (Generation I). On the positive side, these materials have nearly ideal equilibrium thermodynamics, good packing densities, moderate volume expansion and useful sintering properties. Negative aspects that were found include slow kinetics, less-than-theoretical reversible capacities, and impurities in the released hydrogen gas stream. Our current research has focused on developing solutions to these barriers. Two new generations of materials have been investigated. These are Generation II which utilizes solid $TiCl_3$ to catalyze $NaAlH_4$ and Generation III which involves the direct synthesis of catalyzed $NaAlH_4$ from NaH, Al and catalyst precursors.

In-depth rate studies and material analysis were performed on the Generation II materials leading to a comprehensive understanding of the interaction of $TiCl_3$ with $NaAlH_4$ and ultimately the trade-off between improved kinetics and lower hydrogen capacities. These materials also demonstrated better capacities and rates than the earlier Generation I materials. Arrhenius analysis of the rate data made clear that the activation energy is lowered with even low levels of catalyst doping. This clearly points to a catalyst-induced change in hydride decomposition (and probably reformation) mechanisms.

Generation III materials show hydrogen absorption and desorption rates well over an order of magnitude faster than Generation II alanates. In addition, the alanate purification step has been eliminated leading to a radically simplified processing method. This in hand will lead to significantly lower production costs. The direct synthesis technique also eliminates all traces of hydrocarbon impurities in the product hydrogen gas stream. This year's work represents a number of significant advances in the development of practical and inexpensive light-weight hydrogen storage materials.

Introduction

The alkali metal alanates are compounds belonging to the larger class of complex hydrides. In the past, they were known to liberate copious amounts of hydrogen either by direct thermal decomposition or by one-time hydrolysis. However, they were generally considered too irreversible for practical hydrogen storage applications. This was until Bogdanovic et al (Bogdanovic' 1997) demonstrated that the alanate, $NaAlH_4$, would reversible desorb and absorbed hydrogen under relatively mild conditions when doped with Ti-based catalyst. Since that time there has been a growing body of work in characterizing catalyzed alanates, as well as the development of new catalysts and methods of preparation (Bogdanovic' 2000, 2001, Jensen 1999, 2001, Zidan 1999, Zaluska 2000, 2001, Gross 1999, Thomas 1999).

Unlike the interstitial intermetallic hydrides, the alanates release hydrogen through a series of decomposition/recombination reactions:

$$NaAlH_4 \Leftrightarrow 1/3Na_3AlH_6 + 2/3Al + H_2 \Leftrightarrow NaH + Al + 3/2H_2 \qquad \textbf{(Eq.1)}$$

The two combined reactions give a theoretical reversible hydrogen storage capacity of 5.6 wt.%. Previous studies showed that the first reaction will release 1 atm of H_2 at 33°C and the second reaction releases 1 atm of H_2 at 126°C (Bogdanovic' 2000, Gross 2000).

Two areas of progress have been identified as being necessary to develop catalyzed-alanates into a practical material for hydrogen storage for PEM fuel cell vehicle applications:

A) The optimization of the catalyst as to (a) type, (b) doping process and (c) mechanistic understanding.
B) Engineering development and determination of practical properties.

We have employed a parallel approach to address these two areas by working concurrently on the following topics:

- Innovating methods to synthesize the alanates and improve the catalyst doping process to improve both rates and capacity,
- Characterizing relevant material properties of each new generation of material to aid in developing the next generation and to gain a fundamental understanding of the hydrogen absorption and desorption processes,
- Evaluating the behavior of our materials on an engineering scale to ensure that they are on track for eventual commercialization.

The primary goal of this current years work was to resolve potential problems identified last year that would preclude using the alanates for fuel-cell vehicle applications. Previous cycling tests indicated a much lower than expected capacity after the first desorption. Besides this, the use of alkoxide-based Ti and Zr catalysts introduces oxygen and hydrocarbon impurities into the sample which were still present after several cycles. Such impurities could cause irreversible damage to PEM fuel cell catalysts. For this reason we began to investigate a second-generation material which used the inorganic catalyst $TiCl_3$ as well as a purely dry doping process. However, GC-MS analysis indicated that even without using alkoxide-based catalysts the alanate itself contained measurable quantities of residual THF. This residual THF comes from the purification process in which $NaAlH_4$ is dissolved in THF, decanted and then vacuum precipitated. The drawbacks of using solvent-prepared $NaAlH_4$ as the starting material were clear and led us to develop third generation material that employs a direct-dry-synthesis/doping technique. This approach is also being pursued in other laboratories (Bogdanovic' 2001, Zaluska 2001).

Experimental Basics

Crystalline $NaAlH_4$ was made by cryopumping THF from a 1.0M solution of $NaAlH_4$ in THF (Aldrich Chemical No. 40,424-1), followed by vacuum drying with a mechanical and/or turbomolecular pump. Mixtures of $NaAlH_4$ and solid $TiCl_3$ (99.999% Aldrich Chemical No. 51,438-1) were weighed in a purified argon glovebox in the levels of 0.9, 2, 4, 6 and 9 mol% $TiCl_3$. These mixtures were then ball-milled in argon for 3 hours, using a high-energy SPEX® mill and WC balls and milling vial. The powder-to-ball weight ratio was approximately 1:12. Samples were transferred from the milling pot to the reactor vessel in the Ar glovebox. X-ray diffraction (using special airless sample holders) was done before and after milling; in all cases the complete conversion of $TiCl_3$ to NaCl during milling was confirmed.

Dehydriding and hydriding rates and capacities were obtained volumetrically using a Sieverts' apparatus and a cylindrical 316 SS reactor (1.3 cm outer diameter by 0.12 cm wall thickness and length of 12cm) containing about 1.5 g of catalyzed samples. A thermocouple well, in the center of the vessel, allows for accurate temperature measurements during cycling. The reactor was heated externally by an electrical heating tape. Absorption pressure changes were quantified with a calibrated 200 atma pressure transducer and desorption pressures with a 1000 Torr (1.3 atma) Baratron® capacitance manometer. Data were recorded via computer and measurements lasted from minutes to several days, depending on the $TiCl_3$ level and test pressure and temperature conditions.

Hydrogen capacity and rates were measured during the second absorption and desorption half-cycles at 125˚C. During absorption, the applied H_2 pressure was generally in the 80-90 atm range well above the 30-40 atm plateau pressure for $NaAlH_4$ at 125˚C. For the desorption experiments, the back-pressure during $NaAlH_4$ decomposition was kept below 1 atma and during Na_3AlH_6 decomposition below 0.25 atma well below the Na_3AlH_6 plateau pressure of about 2 atma. Hydrogen capacity data are presented as weight % with respect to the total sample weight including the catalyst.

Isothermal Arrhenius analyses were performed as follows: Measurements were started after several hydriding/dehydriding cycles with samples in the fully hydrided condition and cooled to room temperature. The pressure rise from desorption into a known volume, at a given temperature, was measured. The temperature was then increased. The desorption rates were determined at each temperature from the slope of the essentially linear increase in pressure with time. This procedure was continued up to 150˚C. The sample was held at this temperature until the $NaAlH_4$ decomposition step (Eq.1) was finished. The sample was then quickly cooled to 40-60˚C and the Na_3AlH_6 rates determined by the same procedure. The rate data are presented as weight % with respect to the starting alanate weight before doping.

Experimental Results – Generation II Alanates

Our initial studies focused on what we now refer to as Generation I materials (Gross 2000, 2001a, Sandrock 2001a). These consisted of $NaAlH_4$ mechanical mixed with 2 mol% each of liquid $Ti(OBu^n)_4$ and $Zr(OPr)_4$. The use of this formula was based on the observation that combined Ti- and Zr-doping resulted in maximum desorption kinetics for both steps of Eq.1 (Zidan, 1999). Because decomposition of the alkoxides produced organic impurities in the desorbed hydrogen, we redirected activities toward the inorganic catalyst precursor $TiCl_3$. This last year much of our work was performed on Generation II materials (Sandrock 2001b). These were prepared by ball milling solid $TiCl_3$ with solid $NaAlH_4$ (vacuum dried from THF solutions).

Interaction of $TiCl_3$ with $NaAlH_4$

The interaction between $NaAlH_4$ and $TiCl_3$ was investigated by XRD (X-ray Diffraction) (Gross 2001b). Two samples were prepared by ball-milling solid $NaAlH_4$ in argon for 3 hours. One sample was milled together with 9 mol% solid $TiCl_3$. The other was milled without any catalyst. The XRD measurements of these two samples are compared in Figure 1. $TiCl_3$ was not observed. However, NaCl is clearly present. Thus, $NaAlH_4$ and $TiCl_3$ react during the milling process to form NaCl. This result is significant in that it points to the catalyst being composed of a $TiCl_3$ decomposition product probably in the form of Ti metal or an alloy.

Another important observation is that $NaAlH_4$ decomposes to a considerable degree during mechanical milling when $TiCl_3$ is added. This can be seen in the greatly reduced intensities of the $NaAlH_4$ peaks and the presence of reflections from Na_3AlH_6 and Al. This means that the catalytic processes leading to desorption of the $NaAlH_4$, occur even at the relatively low temperatures reached during ball milling.

Capacity Loss with Increasing Catalyst Content

The XRD results showing that $NaAlH_4$ and $TiCl_3$ react during the milling process to form NaCl also explains much of the previously observed capacity loss. The amount of $NaAlH_4$ that is rendered inactive by decomposition into NaCl and Al is proportional to the quantity of added $TiCl_3$. The total reversible hydrogen capacity loss increases with increasing catalyst content (Figure 2). The origin of an additional capacity loss on the order of about 10% below the theoretical level is still not fully understood.

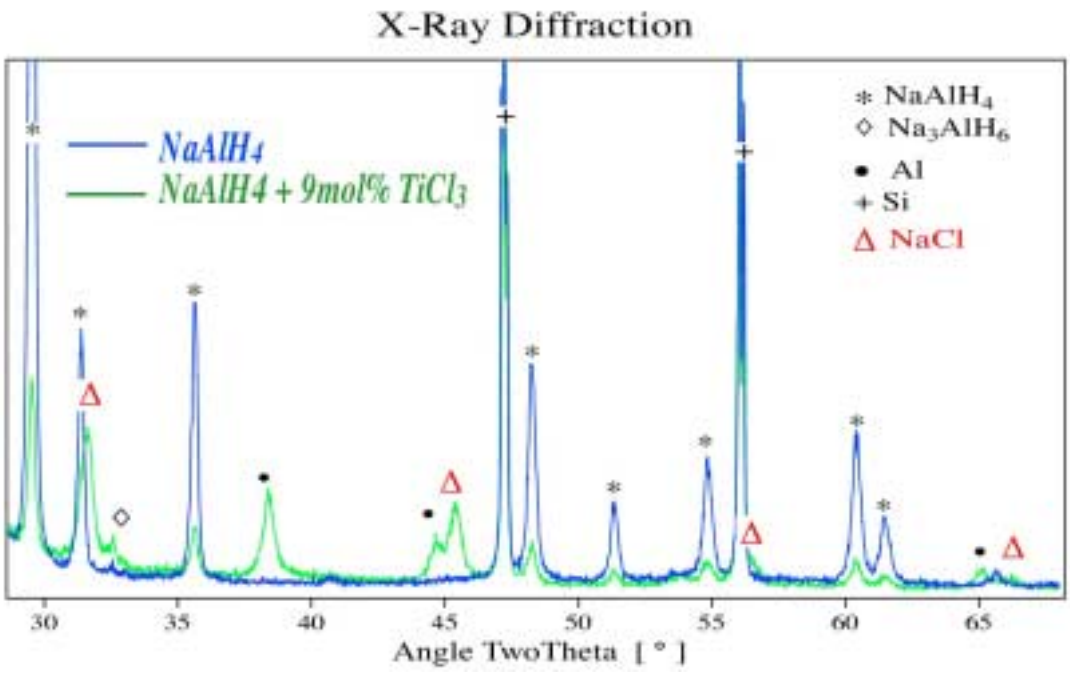

Figure 1 – X-ray diffraction patterns of $NaAlH_4$ after ball milling (green/gray) with $TiCl_3$ catalyst and (blue/black) without catalyst.

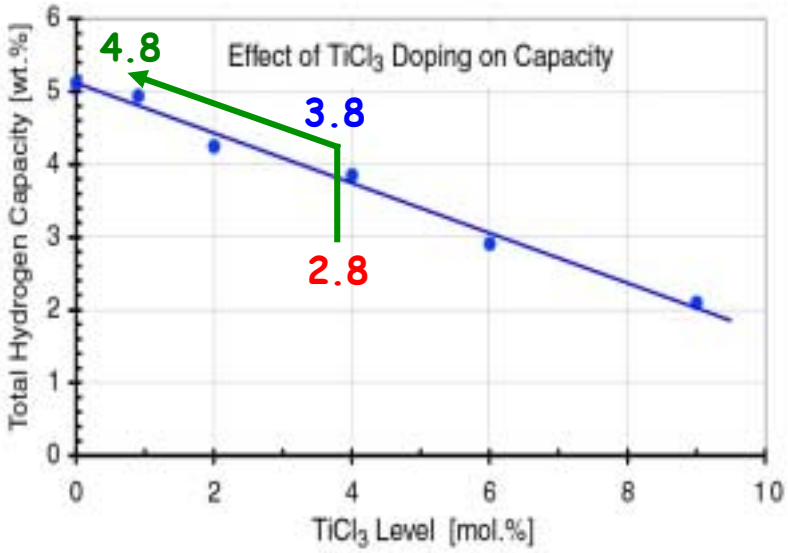

Figure 2 – Reversible hydrogen capacity as a function of $TiCl_3$ content.

Improved Kinetics with Increasing Catalyst Content

Contrary to the generally held view, the rates of hydrogen absorption and desorption are strongly dependent on the level of catalyst doping. Desorption kinetics were measured at different temperatures for $NaAlH_4$ samples doped with 0.9, 2, 4, 6 and 9 mol% $TiCl_3$. An Arrhenius analysis was very effectively applied to the results (next section). The effect of catalyst doping is made clear when the hydrogen desorption rates are plotted versus catalyst content. This is shown in Figure 3 for 125˚C, which is a temperature which will provide hydrogen at greater than atmospheric pressures, as may be required for fuel cell applications. In this case, the desorption rates were calculated from rate constants obtained from the Arrhenius analysis (note, the 9% $TiCl_3$ points were not calculated but rather taken directly from a quasi-isothermal desorption curve). Such an analysis provides a practical way to determine the catalyst doping level required to reach specified desorption rates. Comparing Figures 2 and 3, it is clear that improvements in kinetics with increasing Ti-catalyst-level must ultimately be weighed against the loss of reversible hydrogen capacity. These studies provide the practical tools necessary to choose a reasonable balance between kinetics and capacity.

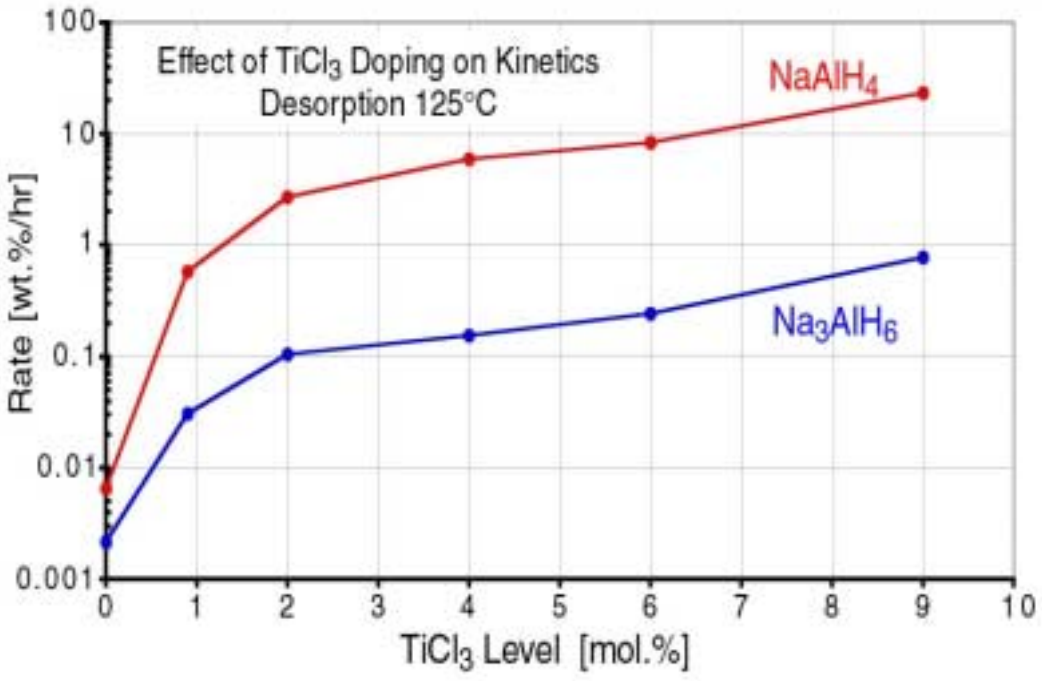

Figure 3 – Rates of hydrogen desorption as a function of $TiCl_3$ content for the decompositions of $NaAlH_4$ and Na_3AlH_6.

Isothermal Kinetic Measurements and Arrhenius Analysis

During the last year we performed isothermal Arrhenius analyses on both the $NaAlH_4$ and Na_3AlH_6 decomposition reactions for the 0, 0.9, 2, 4, and 6 mol% $TiCl_3$ samples. The Arrhenius equation to describe thermally activated chemical process is given by

$$\text{Rate} = k \exp(-Q/RT) \qquad \text{(Eq.2)}$$

where k is the pre-exponential rate constant, Q is the thermal activation energy, R is the gas constant and T is absolute temperature. Thus, an Arrhenius plot consists of plotting ln(rate) vs. 1/T, with the slope of the plot representing the activation energy Q and the 1/T=0 intercept representing the rate constant k. The resultant Arrhenius plots for 0 to 6% $TiCl_3$ are shown in Figures 4 and 5 for $NaAlH_4$ and Na_3AlH_6 decompositions, respectively. All of the data can be represented quite well with an exponential equation of the form Equation 2. These fits have important engineering value by conveniently allowing one to calculate true isothermal kinetics at any temperature and also model non-isothermal operation of hydrogen storage tanks or other commercial processes.

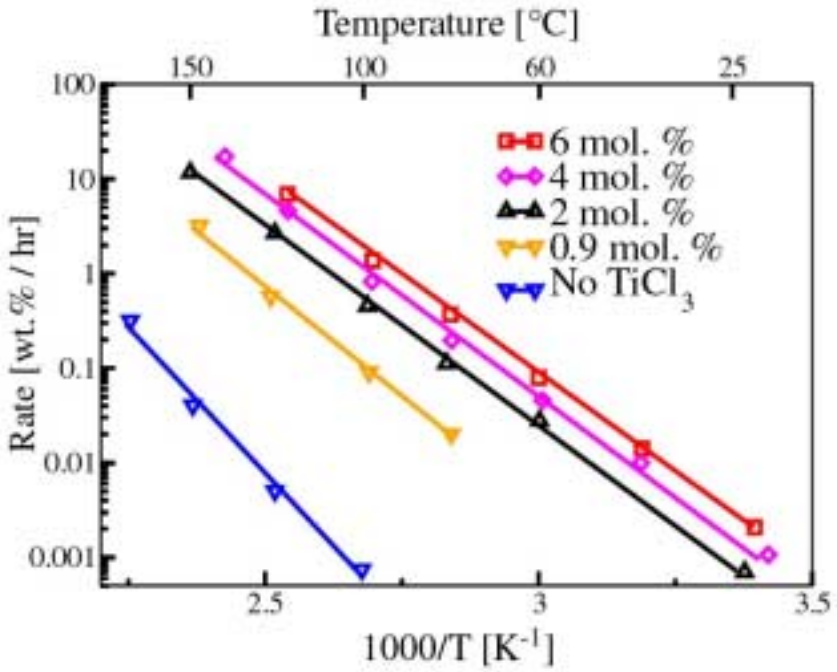

Figure 4 – Arrhenius plot of the hydrogen desorption rates vs. 1/T for the decomposition of $NaAlH_4$.

The effects of catalyst level on the Arrhenius plots are quite dramatic. Note the multiple order of magnitude rate shifts for both the $NaAlH_4$ and Na_3AlH_6 lines as $TiCl_3$ levels are increased (or equivalently the substantial shifts in temperatures for given rates). Let us explore these remarkable differences by examining the Arrhenius parameters Q and k for all the samples evaluated. Q and k are plotted versus $TiCl_3$ level in Figures 6 and 7, respectively. As can be seen in Figure 6, the Q's are nearly equal for the decompositions of both the $NaAlH_4$ and Na_3AlH_6 with 0% $TiCl_3$, but drop to much lower and different levels when even a small amount of catalyst is added (0.9%). This indicates a substantial easing of the thermally activated mechanism. Q then remains virtually constant with $TiCl_3$ level above 0.9%, suggesting no further change in fundamental mechanism after the first small Ti-addition. Figure 7 shows similar decreases of k, including $NaAlH_4$-Na_3AlH_6 differentiation starting with the first small Ti-addition. Unlike Q, however, k increases monotonically with further increases in $TiCl_3$ addition,

and is therefore alone responsible for all the further increases in kinetics above the first 0.9% Ti-addition.

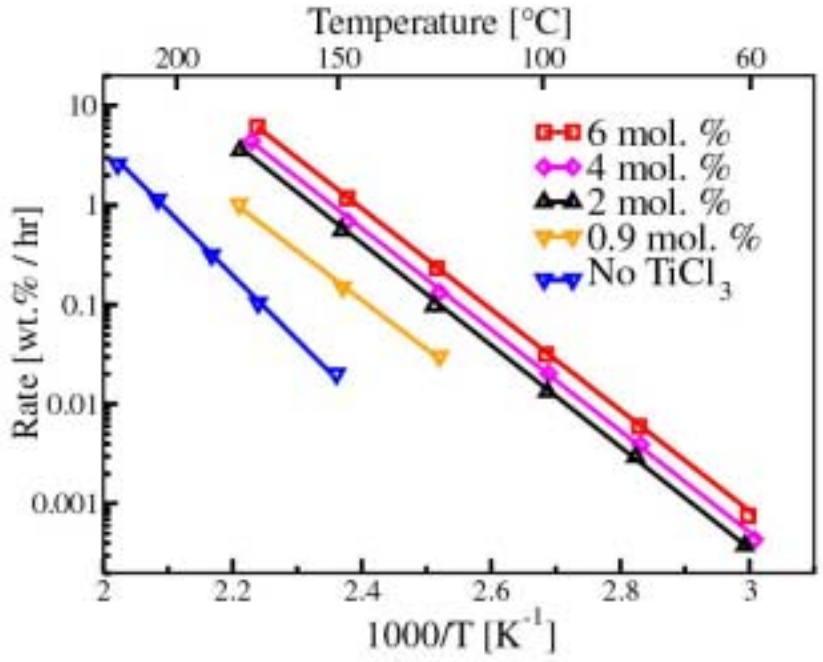

Figure 5 – Arrhenius plot of the hydrogen desorption rates vs. 1/T for the decomposition of Na_3AlH_6.

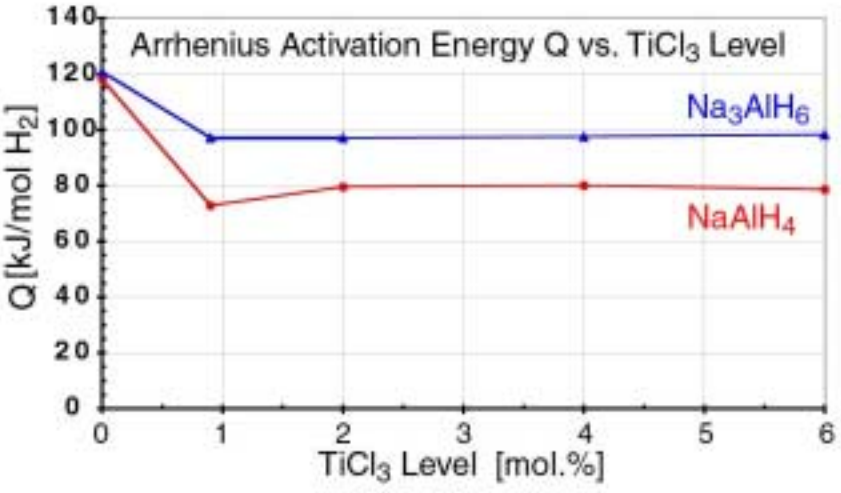

Figure 6 – Activation energy Q as a function of $TiCl_3$ content for the decompositions of $NaAlH_4$ and Na_3AlH_6.

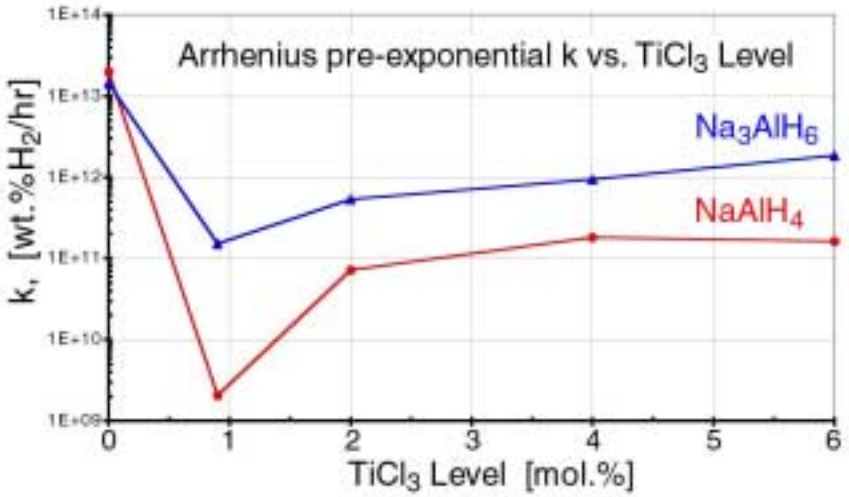

Figure 7 – Pre-exponential factor k as a function of $TiCl_3$ content for the decompositions of $NaAlH_4$ and Na_3AlH_6.

Scaleup Test Bed-2

As a continuation of the engineering activities we reported last year (Gross 2000), a second scaleup test bed was constructed, loaded with 72 g of 4 mol% $TiCl_3$ catalyzed $NaAlH_4$ and evaluated over four complete discharge/charge cycles. This second bed consisted of a 24.5 cm long stainless steel tube 3.17 cm diameter by 0.21 cm wall thickness (Figure 8). These dimensions are perhaps typical of one element one might find in practical vehicular-sized storage system. The intent was to study rate behavior and to model same from combined kinetic and heat transfer points of view. For that reason, two axial thermocouple wells were included (one centerline and one at the half-radius). Thermocouples were placed at top, middle and bottom in each well, and also at equivalent places on the outside diameter (total of nine measuring thermocouples). The instrumented reactor, wrapped with electrical heating tape, was evaluated on a new apparatus built for that purpose (Figure 8). It was designed for isobaric charging, followed by non-isobaric discharging into a large calibrated volume. All data was logged via computer for subsequent analysis.

Charging runs were done at 125˚C at 60, 75 and 90 atm applied hydrogen pressure. For comparison purposes, an additional charging run was done at 100˚C and 90 atm. Discharging runs were performed at 80, 100, 125 and 150˚C. As only one example, the 100˚C discharge curve is shown in Figure 9. About 2.2 wt.% H_2 is released in 3 hours, representing decomposition of the $NaAlH_4$ phase (first step). The decomposition of the Na_3AlH_6 then begins sequentially, but that is a much slower process. The temperature was then increased to 150˚C to complete the Na_3AlH_6 decomposition. A large amount of such data was generated as is now being analyzed. The marks placed on the reactor (Figure 8) were used as reference points to determine if any expansion deformation took place during the cycling. No measurable deformation was found.

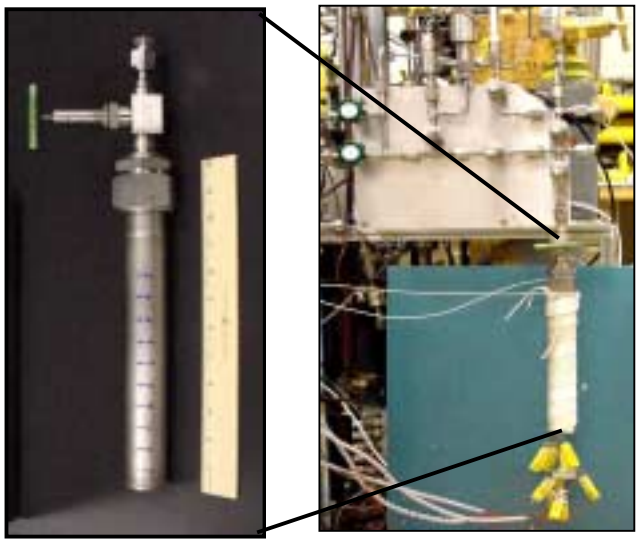

Figure 8 – Scaled-up Bed-2 and test stand showing control manifold, tape heater and axial thermocouples.

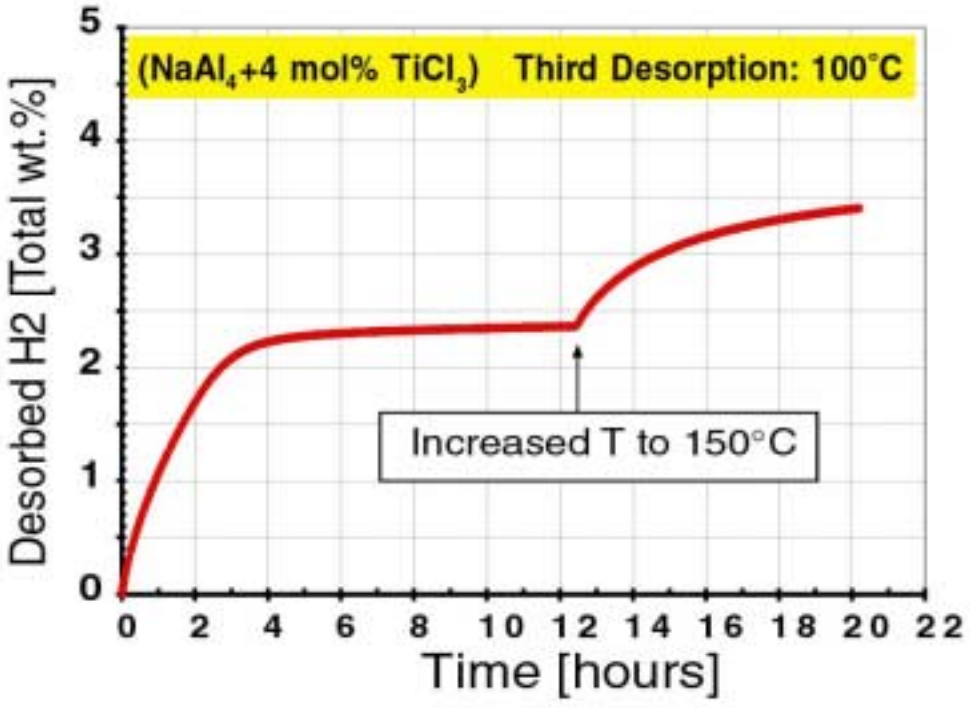

Figure 9 – Third hydrogen desorption from scaled-up test Bed-2.

The capacity (3.4 total wt.% H_2 in Figure 9) was somewhat disappointing, but an expected result of the inherent losses that result from the Generation II catalyzing reaction (reaction of the $TiCl_3$ catalyst precursor with some of the $NaAlH_4$ to form NaCl). During the evaluation of Bed-2 an

improved catalysis process (Generation III) was developed that may reduce this problem (see Figures 11 and 12 and discussion which follows). Therefore no more work will be done on Bed-2 and a new scaled-up reactor Bed-3 will be evaluated with Generation III catalyzed alanate.

Experimental Results – Generation III Alanates

While residual gas analysis (Figure 10) of the Generation II materials showed significantly reduced levels of hydrocarbon contaminant compared to the Generation I alanates, trace levels of impurities remained. These were identified by GC/MS analyses as residual THF (and pentane if used for precipitation) remaining from the $NaAlH_4$ purification process. This and the lower than desired reversible capacities lead to the development of a direct synthesis/catalyst doping technique that is now used to produce Generation III alanates. These materials are prepared directly from the decomposition products and catalyst. No solvents whatsoever are used in this process. As a result the desorbed hydrogen shows no hydrocarbon contaminants (Figure 10). Only trace levels of H_2O and CO from the vacuum system are observed. Perhaps the most significant impact of these results is the fact that catalyzed alanates can now be produced under relatively mild conditions without solvents, thus substantially reducing raw material and production costs.

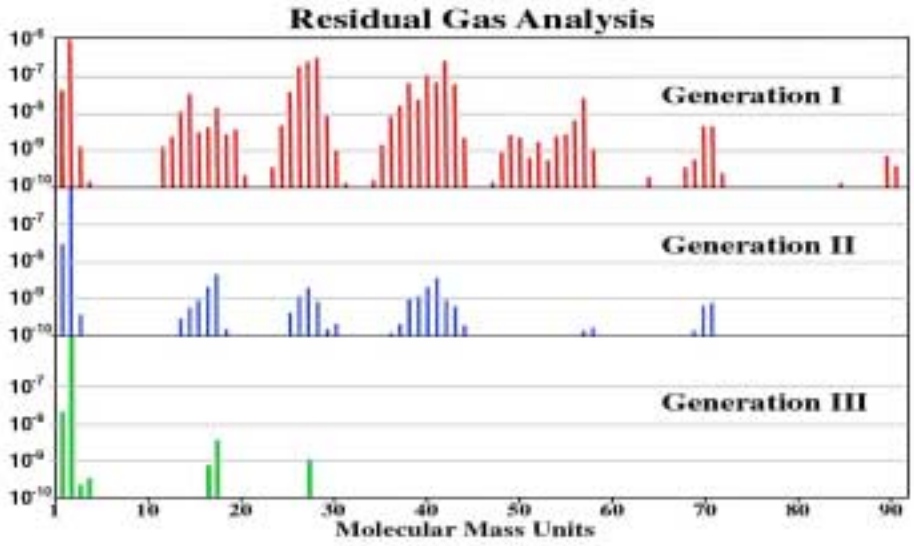

Figure 10 – Residual desorbed gas spectra from samples of Generation I, II and III materials.

An added benefit is that the starting composition of these Generation III materials can be tailored to reduce inactive by-products (namely Al) of the catalyst doping process. Depending on the level of catalyst employed this can significantly improve the reversible hydrogen capacity.

In addition to these remarkable improvements, the Generation III materials also surprised us by having astonishingly rapid kinetics. The absorption and desorption kinetics of the Generation III alanates are compared with Generation II materials in Figures 11 and 12 respectively. The

absorption rates are some 20 times faster for the Generation III alanates and they are about 10 times better in desorption.

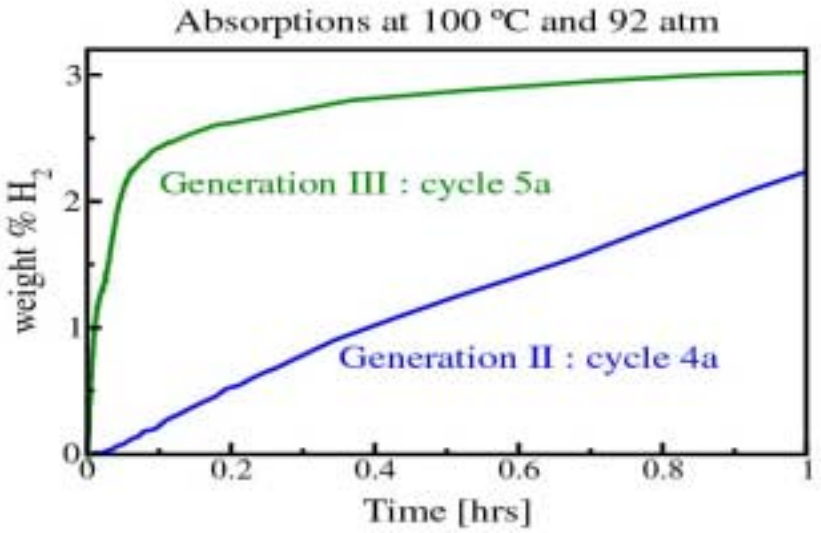

Figure 11 – A comparison of hydrogen absorption by samples of Generation II and III materials (both 4 mol% catalyst).

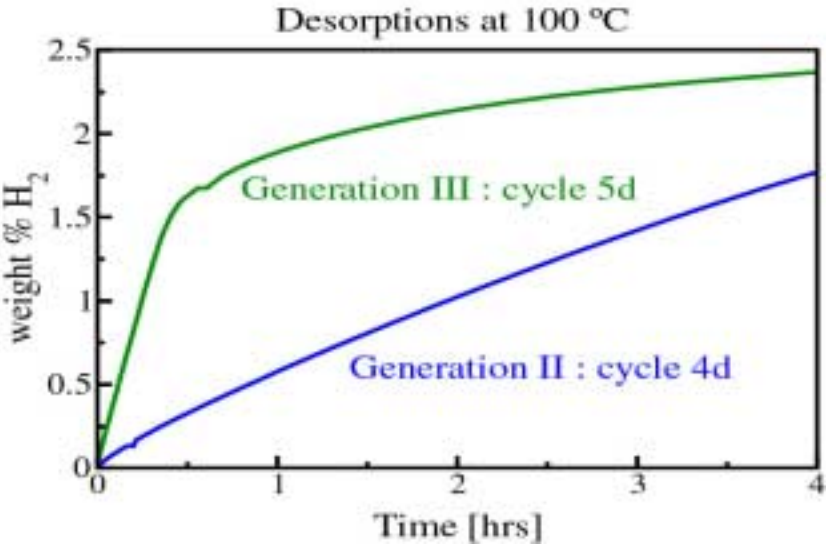

Figure 12 – A comparison of hydrogen desorption from samples of Generation II and III materials (both 4 mol% catalyst).

An important effect, which was not observed in previous generations of materials, is that the kinetics improved dramatically with the first couple of cycles. This is somehow an activation process that is likely a result of the catalyst's initial interaction with the alanate and particle size reduction. Figure 13 shows the first two hydrogen absorption cycles (100 atm H_2) for Generation III alanate doped with 1 mol% catalyst. The absorption rate in the 2nd cycle is significantly better than even the 4 mol% $TiCl_3$ doped Generation II materials and the same is true for desorption. This is significant because high rates may now be achieved with much lower catalyst loading.

This, in turn, means that higher reversible capacities can now be obtained. In this case the sample reversibly absorbed and desorbed 4.8 wt.% hydrogen.

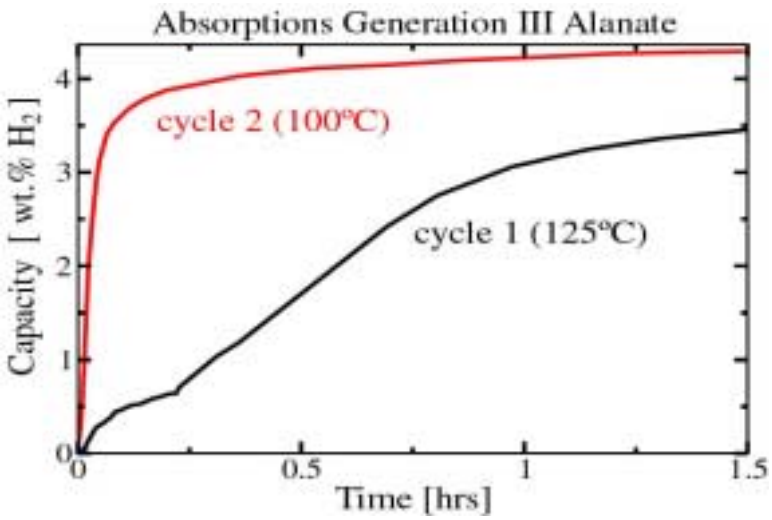

Figure 13 – Activation effect of first two cycles on Generation III materials (1 mol% catalyst).

Conclusion

The advances that have been achieved thus far can be appreciated by revisiting Figure 2. Generation I materials had relatively low true capacities (2.8 wt.% H_2) due in large part to the excess weight of the alkoxide catalyst precursors (22 wt.% for 4 mol% catalyst). Initial improvements (3.8 wt.% H_2) were accomplished by switching to the inorganic solid catalyst $TiCl_3$. Using Generation II alanates, we demonstrated that the reaction between $TiCl_3$ and the alanate leads to a trade-off between increased kinetics and loss of capacity as the catalyst level is increased. On moving from Generation II to Generation III materials the capacity was improved to 4.8 wt.% H_2 simply by reducing the level of catalyst loading required to achieve the same hydrogen sorption rates. In summary, the latest generation of catalyzed alanates has resolved the issue of hydrogen gas contamination and offer rapid kinetics and high capacities in a material that should be substantially less costly and complicated to produce than previous generations.

Future work

Our future work is now focused on further improving the capacity and kinetics of the Generation III alanates. These materials will be examined through extensive cycle-life and scale-up studies. We are also expanding the new synthesis and catalyst doping techniques to other complex hydrides. This includes investigating Mg-based complex hydrides in collaboration with the University of Geneva.

An important observation was made during recent studies. Millimeter-size aluminum flakes were completely consumed by the alanates during absorption. This is an area of safety concerns

that many researchers and commercial entities may not have considered. There is a strong possibility that cycling the alanates in aluminum-based vessels will cause erosion of the vessel walls and ultimately lead to vessel failure. We are currently investigating the interaction of the catalyzed alanates with various containment vessel materials.

Acknowledgements

We wish to acknowledge the valuable collaboration of C. Jensen of the University of Hawaii. We thank D. Meeker of SNL for his expert technical help in all aspects of the experimental measurements and Ken Stewart of SNL for all of his contributions in developing our experimental equipment.

Funding is provided by the U.S. Department of Energy, Office of Power Technologies, Hydrogen Program Office under contract DE-AC36-83CH10093. Sandia is a multi-program laboratory operated by Sandia Corporation, a Lockheed Martin Company, for the U.S. Department of Energy under contract DE-AC04-94-AL85000.

References

Bogdanovic', B. and Schwickardi, M. 1997. "Ti-doped alkali metal aluminum hydrides as potential novel reversible hydrogen storage materials," *J. Alloys and Compounds*, **253**:1.

Bogdanovic', B., Brand, R.A., Marjanovic', A., Schwikardi, M., and Tölle, J. 2000. "Metal-doped sodium aluminum hydrides as potential new hydrogen storage materials," *J. Alloys and Compounds*, **302**:36.

Bogdanovic B., Schwickardi M. 2001. "Ti-doped $NaAlH_4$ as a hydrogen-storage material – preparation by Ti-catalyzed hydrogenation of aluminum powder in conjunction with sodium hydride," *Applied Physics A*, 72 (#2):221.

Gross, K.J., Guthrie, S.E., Takara, S., and Thomas, G.J. 1999. "*In situ* X-ray diffraction study of the decomposition of $NaAlH_4$," *J. Alloys and Compounds*, **297**:270.

Gross, K.J., Thomas, G.J., and Sandrock, G., 2000. "Hydride development for hydrogen storage," in *Proceedings U.S. DOE Hydrogen Program Review*, NREL/CP-570-26938,452. San Ramon, CA.

Gross, K.J., Thomas, G.J., and Jensen, C.M., 2001a. "Catalyzed Alanates for Hydrogen Storage," In *Proceedings of the International Symposium on Metal Hydrogen Systems*, Noosa, Australia, Oct. 2000.

Gross, K.J., Sandrock, G., and Thomas, G.J. 2001b. "Dynamic In Situ X-ray Diffraction of Catalyzed Alanates," In *Proceedings of the International Symposium on Metal Hydrogen Systems*, Noosa, Australia, Oct. 2000.

Jensen, C.M., Zidan, R.A., Mariels, N., Hee, A.G., and Hagen, C. 1999. "Advanced titanium doping of sodium aluminum hydride: segue to a practical hydrogen storage material?," *Int. J. Hydrogen Energy*, **24**:461.

Jensen C.M., Gross K.J. 2001. "Development of Catalytically Enhanced Sodium Aluminum Hydride as Hydrogen Storage Material," *Applied Physics A*, 72(#2):221.

Sandrock, G., Gross, K., Thomas, G., Jensen, C., Meeker, D. and Takara, S. 2001a. "Engineering considerations in the use of catalyzed sodium alanates for hydrogen storage," In *Proceedings of the International Symposium on Metal Hydrogen Systems*, Noosa, Australia, Oct. 2000.

Sandrock, G., Gross, K., Thomas, G. 2001b. "Effect of Ti-catalyst content on the reversible hydrogen storage properties of the sodium alanates," submitted *J. Alloys and Compounds*.

Thomas, G.J., Guthrie, S.E., and Gross, K. 1999. "Hydride development for hydrogen storage," in *Proceedings U.S. DOE Hydrogen Program Review*, NREL/CP-570-26938,452. Denver CO.

Zaluska, A., Zaluski, L., and Ström-Olsen, J.O. 2000. "Sodium alanates for reversible hydrogen storage," *J. Alloys and Compounds*, **298**:125.

Zaluska A., Zaluski L., Strom-Olsen J.O. 2001. "Structure, catalysis and atomic reactions on the nano-scale: a systematic approach to metal hydrides for hydrogen storage", *Applied Physics A*, 72(#2):157.

Zidan, R.A., Takara, S., Hee, A.G., and Jensen, C.M. 1999. "Hydrogen Cycling Behavior of Zirconium and Titanium-Zirconium Doped Sodium aluminum Hydride", *J. Alloys and Compounds*., **285**:119.